UDC 539.4

Strength Improvement of Ferritic/Martensitic T91 Steel by Cross Wedge Rolling at Different Austenitizing Temperatures

T. He,[1] L. Min, and H. J. Liu

Department of Mechanical engineering, Shanghai University of Science Technology, Songjiang, Shanghai, China

[1] hetao@sues.edu.cn

Cross wedge rolling (CWR) is a forming technique wherein the processed material microstructure is controlled by the processing temperature. The initial results on CWR-processed T91 steels at different austenitizing temperatures are discussed with the microstructure analysis by various characterization techniques, such as the optical and scanning electron microscopies. The processed T91 specimens were much harder than water-quenched ones, their hardness being independent of the ausforming temperatures despite their microstructural differences.

Keywords: cross wedge rolling, ausforming, ferritic/martensitic T91 steel, deformation.

Introduction. Chromium bearing ferritic-martensitic steels were originally designed for conventional fossil power plants. In the 1970s, they were used for high-temperature structural applications in the core of faster reactors in the developed countries [1]. T91 steel has a low production cost and excellent mechanical, physical, and chemical properties. This makes it extremely attractive for pressure vessel applications and for the fossil power or petrochemical industry piping systems [2].

According to Fig. 1, cross wedge rolling (CWR) is considered as a novel plastic deformation process. In order to produce parts such as stepped axes and shafts, the action of wedge shape dies and moves tangentially relative to each other [3]. The benefits of CWR are significant when compared with other conventional forming processes, such as high productivity, great material utilization, good mechanical properties, reduced energy consumption, as well as no harm to the environment [4, 5].

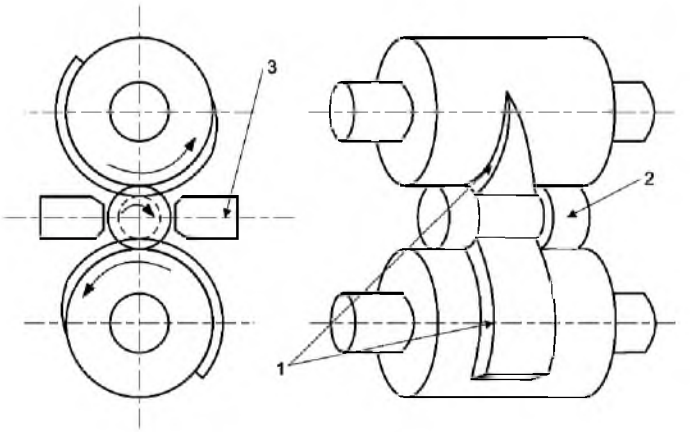

Fig. 1. Schematic of CWR with two rolls: (*1*) rolls with wedge, (*2*) billet, and (*3*) guide plates.

In recent years, CWR is used for processing of various types of materials. Among them, Silva et al. [6] studied the behavior of the microalloyed steel DIN 38MnSiVS5. Çakırcalı et al. [7] carried out experiments to examine the deformation and fracture of

Ti6A14V alloy. To test the microstructure evolution of 40MnV steel, Wang et al. [8] performed the respective experiments. Zhang et al. [9] investigated the effect of cross wedge rolling on the microstructure of GH4169 alloy, while He et al. [10] investigated the deformation of Inconel 718 alloy. Due to the advantages that resulted from the study on T91 steel by CWR, the application prospects are significant. Because temperature is the influencing factor for the CWR deformation and microstructure evaluation, the rolling experiments of T91 at different temperatures were conducted. Subsequently, the microstructure evaluation of T91 is discussed, and the mechanical properties at different temperatures are also assessed.

1. **Experiment**. Table 1 listes the chemical composition of the as-received (AR) T91 alloy in wt.%. Initially, the as-received T91 was hot-forged and then heat-treated by the standard normalization and tempering procedures. Then, the CWR was carried out on CWR mill H500. The main properties of rolling process are as follows: forming angle of $\alpha = 35°$, stretching angle of $\beta = 5.5°$, area reduction of $\Delta A = 66\%$, and rotating speed of $n = 10$ rpm. Since temperature is the crotical factor controlling the microstructure and mechanical properties of T91 alloys, four different rolling temperatures of 900, 1040, 1100, and 1200°C were selected. Billets were water-quenched prior to processing at elevated temperatures.

T a b l e 1

Chemical Composition (wt.%) of the As-Received T91 Alloy

Cr	Mo	V	Mn	C	Si	Cu	Ni	Al	Nb	N	P	S
8.35	0.925	0.21	0.44	0.095	0.43	0.06	0.32	0.008	0.079	0.042	0.013	0.005

After rolling, small circular specimens with $\varnothing 7 \times 5$ mm were cut for optical observation, scanning electron microscopy, and hardness tests. The specimens were mechanically polished conforming to the standard procedure and etched prior to the optical observation. By using an LM 300AT microhardness tester, the hardness for the thermal stability study was measured based on a 2.9 N (300 g) loading time force of 13 s using a pyramidal shape diamond indenter. the scanning electron microscopy (SEM) was performed on an FEI Quanta 600 microscope operating at acceleration voltage of 20 kV and working distance of 10 mm. At acceleration voltage of 20 kV and working distance of 10 mm, an FEI Quanta 600 microscope was used to perform SEM.

2. **Results and Discussion**.

2.1. ***Microstructure of AR T91***. Figure 2 shows the microstructure of AR T91. The initial microstructure of the material is a typical tempered martensitic lath structure with carbides at the prior austenite grain boundaries (PAGB) and lath boundaries. As reported by Song et al. [11], similar microstructure has been frequently observed in different T01 alloy batches. In the optical microscopic image, the white block was observed as sporadic of ferritic phase. These phases contribute to a total volume fraction of less than 5%. The ferrite phase is typically formed at a very slow cooling rate. The prior austenite grain size is about 20 μm according to Fig. 2b. The bundles of tempered martenstic laths are the dark features in the SEM image, which are formed during the tempering process through merging the fine martensites with a similar habit plane (also called packet of martensite).

2.2. ***Microstructure Evaluation of T91 Formed by CWR at Different Temperature***. Figure 3 presents the optical micrographs of the T91 steel deformed at 900 and 1040°C, with a fine austenite grain structure, while those deformed at 1100 and 1200°C have a coarse structure, which appears at the temperatures above 1100°C. The grain structure was elongated along the longitudinal direction. According to Fig. 4a and b SEM images, the deformed PAGBs are frequently observed, confirming the previous observation that the

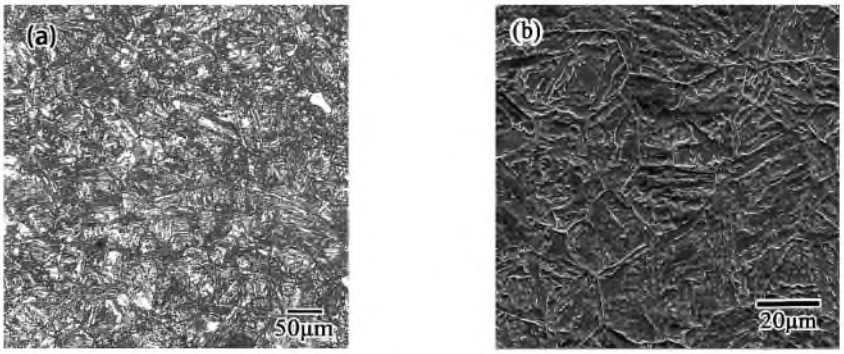

Fig. 2. Tempered martensitic structure of the AR T91 steel: (a) optical microscopy of a typical tempered martensitic lath structure; (b) SEM images of the as received T91 steel observed.

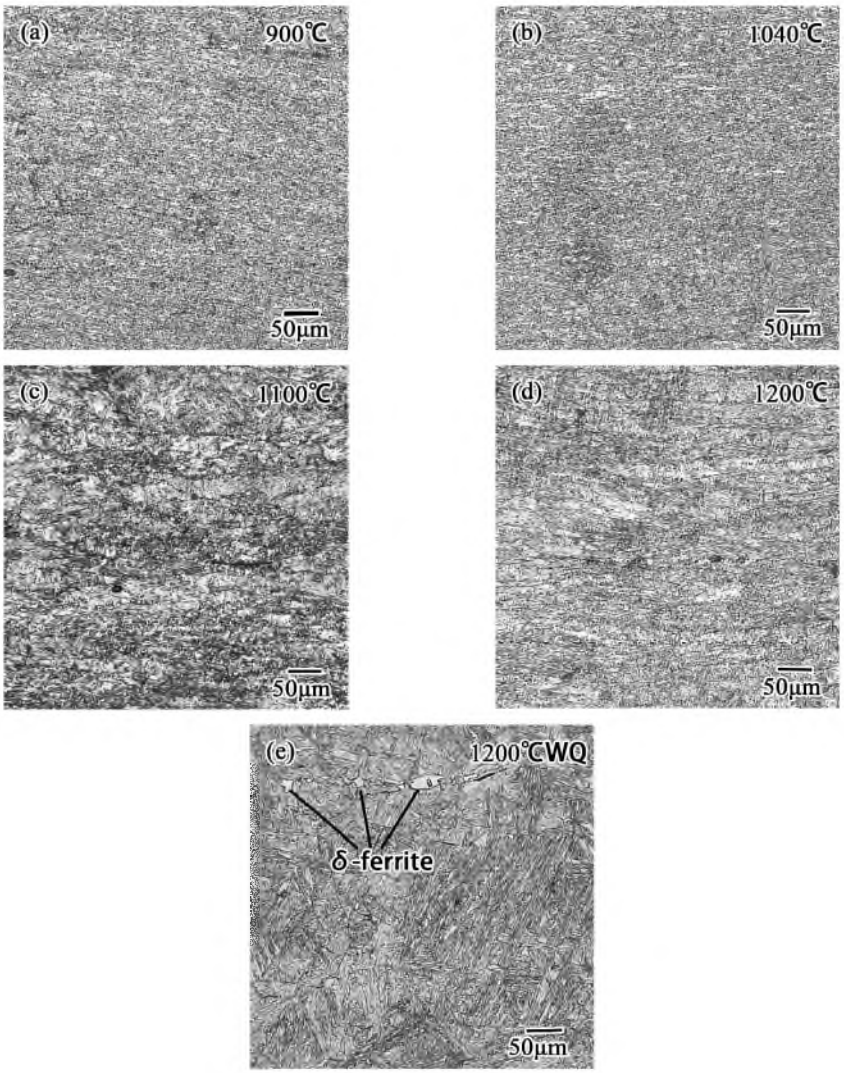

Fig. 3. Deformed microstructure at different austenitizing temperatures (OP), T91 deformed at 900 (a) and 1040℃ (b) show a fine structure and coarsen structure was revealed after deformed at 1100 (c) and 1200℃ (d). The water-quenched materials (e) reveal large grain size of prior austenite grain boundaries and the presence of δ-ferrite at the PAGB.

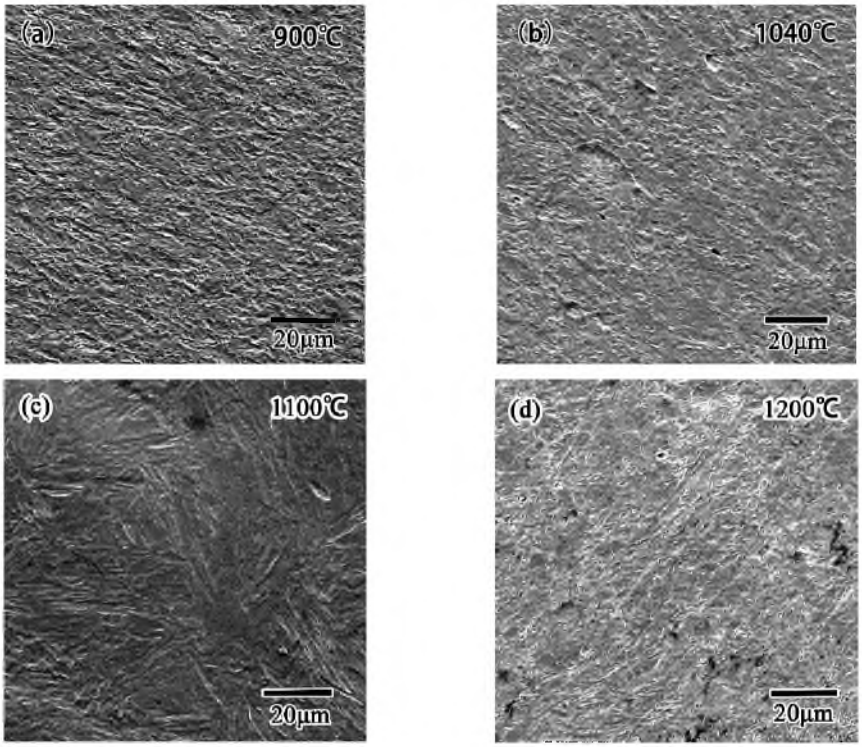

Fig. 4. SEM images of the deformed structure of T91 steel in the longitudinal plane. Deformed PAGBs are observed in the 900 and 1040℃ materials while no significant PAGBs are observed in 1100 and 1200℃ due to the large grain size.

initial austenite grain boundaries elongated along the longitudinal direction. In contrast, due to the large size of the initial austenite grain, no PAGBS were found in Fig. 4c and d, and no elongated structure was observed in the WQ T91 steel. Instead, δ-ferrite was observed at the PAGBs as the white block, which can potentially reduce the creep strength of T91 steel described by Kobayashi et al. [12]. However, after 30 min of normalization at a temperature above 1100°C, this reduction can be eliminated.

Discontinues PAGBs were observed in the transverse plane as shown in Fig. 5, indicating that the PAGBs were partially decomposed during the high-temperature deformation process. Additionally, according to Song et al. [11], similar results have also been observed in an equal channel angular extrusion (ECAE) processed T91 steels. They observed that the PAGBS decompose after up to three passes of high-temperature ECAE. The grain size of the initial austenite observed in the transverse plane is smaller than that observed in the longitudinal plane, indicating that during the ausforming process, a pronounced texture can be formed.

2.3. ***Mechanical Properties of T91 Formed by CWR***. Figure 6 shows the mechanical properties of T91 formed by CWR. Based on Fig. 6a, the average value of hardness of T91 at different temperatures is as follows: 215 HV for the AR material, 419 HV for the non-rolled parts, and 473, 478, 479, and 482 HV for each of the rolled parts, respectively. The rolled material hardness is higher by about 15% than that of the the unrolled one, especially in the AR material, which is more than twice higher. The AR material is typically a tempered martensite structure, which is commonly softer than the non-rolled part. The non-rolled part is a martensite structure quenched at the initial elevated temperature. The solid solution of carbon atoms in martensite can cause asymmetrical distortion of the crystal structure, thus, impeding the mobile dislocation and significantly strengthening the materials

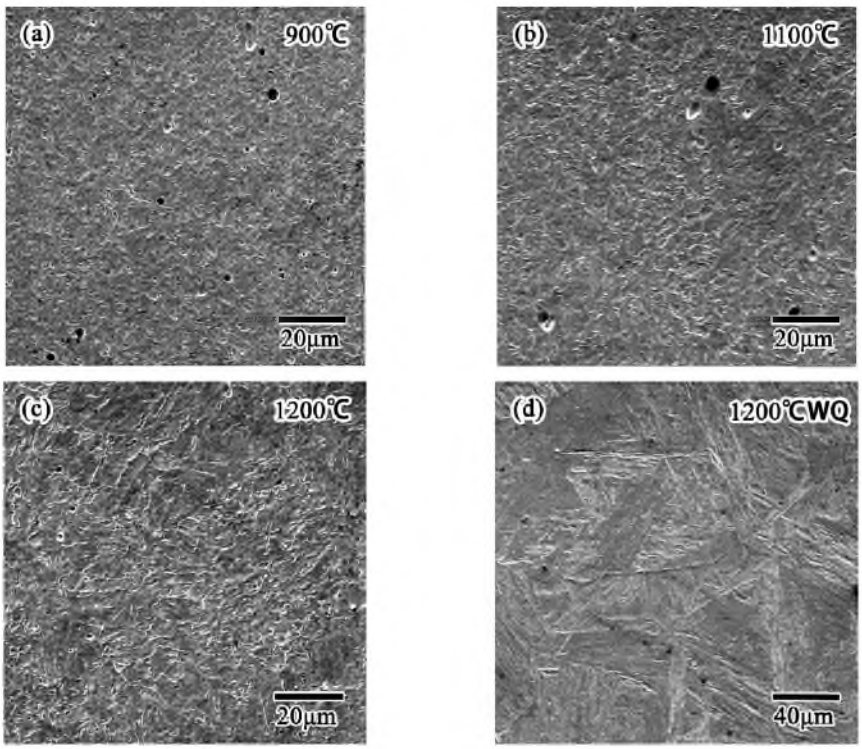

Fig. 5. SEM images of deformed structure of T91 steel observed in the transversal plane. The grain size of the initial austenite grain is smaller. Discontinuous PAGBs are observed, which may indicate the decomposition of PAGBs.

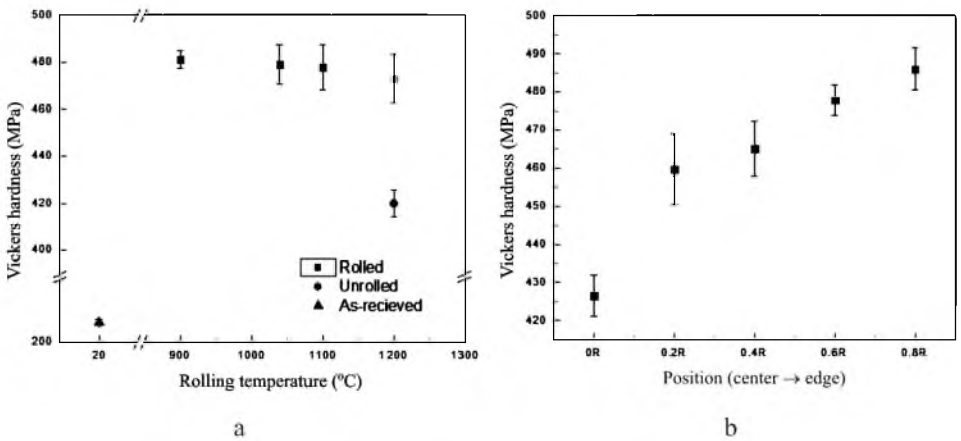

Fig. 6. (a) Hardness evolution of ausformed T91 steel at different temperatures; (b) position depending on as-processed rod radius.

[13]. Both the packet size and block width of martensites decrease during the ausforming process [14]. As compared to the size effect of the long and thick martensite, the thinner and shorter martensite can be highly strengthened.

Figure 6b exhibits that at 900°C, the average value of hardness of T91 decreased from the edge to center location, the maximum value being 486 HV, and the minimum one being 426 HV. This is mainly due to the decrease in deformation from the edge to the center,

leading to the edge grain size being smaller than the centers. Different ausforming results obtained are due to the shear stress differences from the surface to the center. A smaller packet size of martensite is attributed to a higher shear strength during ausforming, thus, leading to a higher hardness. It is also observed that, in comparison to the non-rolled part, the central part has a lower hardness and exhibits zero shear stresses.

Conclusions

1. The mechanical properties of ausformed T91 by CWR are apparently higher than hose of water-quenched T91, especially the AR one. The novel deformation technology has the ability to enhance the material strength.

2. The T91 steel specimens deformed at 900 and 1040°C have a fine structure, while those deformed at 1100 and 1200°C have a coarse structure. The grain structure is elongated along the longitudinal direction.

3. With a temperature increase from 900 to 1200°C, the mechanical properties deteriorate from the edge position to the center one, while the center hardness is almost equal to that of water-quenched T91.

Acknowledgments. This study has been perfomed within framework of the project ZKL-PR-200305 entitled "T91 Shaft Formed by Cross Wedge Rolling," E3-0507-16-0201-16XKCZ01 entitled "Discipline Construction of Mechanical Engineering" and 16030501200 entitled "Research on Key Technologies of Underwater Vehicles for Deep-sea Oil and Gas Fields." We wish to thank X. H. Zhang, M. Song, and L. B. Hang for discussions and advice, which resulted in significant improvements. The provision of microscopes at the Microscopy and Imaging Center at Texas A&M University is also gratefully acknowledged.

1. R. W. Swindeman, M. L. Santella, P. J. Maziasz, et al., "Issues in replacing Cr–Mo steels and stainless steels with 9Cr–1Mo–V steel," *Int. J Pres. Ves. Pip.*, **81**, No. 6, 507–512 (2004).
2. M. J. Cohn, J. F. Henry, and D. Nass, "Fabrication, construction, and operation problems for grade 91 fossil power components," *J. Press. Vess. – T. ASME*, **127**, No. 2, 197–203 (2005).
3. Z. H. Hu, X. H. Xu, and D. Y. Sha, *The Principles, Process and Machines of Helical Rolling, and Cross Wedge Rolling* [in Chinese], Metallurgical Industry Press, Beijing (1985).
4. X. P. Fu and T. A. Dean, "Past developments, current applications and trends in the cross wedge rolling process," *Int. J. Mach. Tool. Manu.*, **33**, No. 3, 367–400 (1993).
5. Z. Pater, "Theoretical method for estimation of mean pressure on contact area between rolling tools and workpiece in cross wedge rolling processes," *Int. J. Mech. Sci.*, **39**, No. 2, 233–243 (1997).
6. M. L. N. Silva, G. H. Pires, and S. T. Button, "Damage evolution during cross wedge rolling of steel DIN 38MnSiVS5," *Proc. Eng.*, **10**, 752–757 (2011).
7. M. Çakırcalı, C. Kılıçaslan, M. Güden, et al., "Cross wedge rolling of a Ti6Al4V (ELI) alloy: the experimental studies and the finite element simulation of the deformation and failure," *Int. J. Adv. Manuf. Technol.*, **65**, 1273–1287 (2012).
8. M. T. Wang, X. T. Li, M. H. Jiang, and F. S. Du, "Numerical simulation and modeling of hot deformation microstructure evolution of a non-quenched and tempered steel in cross wedge rolling," *Trans. Mater. Heat Treat.*, **34**, 168–172 (2013).
9. N. Zhang, B. Y. Wang, and J. G. Lin, "Effect of cross wedge rolling on the microstructure of GH4169 alloy," *Int. J Min. Met. Mater.*, **19**, No. 9, 836–842 (2012).

10. T. He, B. Y. Wang, and Z. H. Hu, "Thermal mechanical coupled simulation of Inconel 718 alloy cross wedge rolling," *J. Plast. Eng.*, **15**, 157–159 (2008).
11. M. Song, R. Zhu, D. C. Foley, et al., "Enhancement of strength and ductility in ultrafine-grained T91 steel through thermomechanical treatments," *J. Mater. Sci.*, **48**, No. 21, 7360–7373 (2013).
12. S. Kobayashi, K. Sawada, T. Hara, et al., "The formation and dissolution of residual δ ferrite in ASME Grade 91 steel plates," *Mater. Sci. Eng. A*, **592**, 241–248 (2014).
13. H. Bhadeshia and R. Honeycombe, *Steels: Microstructure and Properties*, Butterworth–Heinemann (2011).
14. G. Miyamoto, N. Iwata, N. Takayama, and T. Furuhara, "Mapping the parent austenite orientation reconstructed from the orientation of martensite by EBSD and its application to ausformed martensite," *Acta Mater.*, **58**, No. 19, 6393–6403 (2010).

Received 30. 08. 2016